European Journal of Medicinal Chemistry 125 (2017) 1088–1097

Contents lists available at ScienceDirect

European Journal of Medicinal Chemistry

journal homepage: http://www.elsevier.com/locate/ejmech

Research paper

# Rational design of nitrofuran derivatives: Synthesis and valuation as inhibitors of *Trypanosoma cruzi* trypanothione reductase

D.G. Arias [a, b], F.E. Herrera [b], A.S. Garay [b], D. Rodrigues [b], P.S. Forastieri [c], L.E. Luna [c], M.D.L.M. Bürgi [b], C. Prieto [b], A.A. Iglesias [a, b], R.M. Cravero [c], S.A. Guerrero [a, d, *]

[a] Instituto de Agrobiotecnología del Litoral (CONICET-UNL), Argentina
[b] Facultad de Bioquímica y Ciencias Biológicas, Universidad Nacional del Litoral, Argentina
[c] Instituto de Química Rosario (CONICET) - FCByF- Universidad Nacional de Rosario, Argentina
[d] Facultad Regional Santa Fe, Universidad Tecnológica Nacional (UTN), Argentina

ARTICLE INFO

*Article history:*
Received 1 August 2016
Received in revised form
28 September 2016
Accepted 23 October 2016
Available online 24 October 2016

*Keywords:*
Trypanosoma cruzi
Trypanothione
Nitroheterocycle drugs
Nifurtimox

ABSTRACT

The rational design and synthesis of a series of 5-nitro-2-furoic acid analogues are presented. The trypanocidal activity against epimastigote forms of *Trypanosoma cruzi* and the toxic effects on human HeLa cells were tested. Between all synthetic compounds, three of thirteen had an $IC_{50}$ value in the range of Nfx, but compound **13** exhibited an improved effect with an $IC_{50}$ of 1.0 ± 0.1 μM and a selective index of 70 in its toxicity against HeLa cells. We analyzed the activity of compounds **8**, **12** and **13** to interfere in the central redox metabolic pathway in trypanosomatids, which is dependent of reduced trypanothione as the major pivotal thiol. The three compounds behaved as better inhibitors of trypanothione reductase than Nfx (*Ki* values of 118 μM, 61 μM and 68 μM for **8**, **12** and **13**, respectively, compared with 245 μM for Nfx), all following an uncompetitive enzyme inhibition pattern. Docking analysis predicted a binding of inhibitors to the enzyme-substrate complex with binding energy calculated in-silico that supports such molecular interaction.



## 1. Introduction

The unicellular parasite *Trypanosoma cruzi* is the causative agent of Chagas' disease. As aerobic organisms, this parasite and all trypanosomatids, are inevitably exposed to many reactive oxygen and nitrogen species (ROS, and RNS respectively), namely superoxide anions, hydrogen peroxide, peroxynitrite and myeloperoxidase products. These chemical species are generated during host defence reaction and also as by-products of aerobic metabolism. The ability of trypanosomatids to cope with such oxidative stress conditions appears noticeably weak; because even when they possess an iron-containing superoxide dismutase [useful to scavenge phagocyte-derived superoxide anions, see Ref. [1]], they lack catalase and have a glutathione peroxidase-like system that exhibits low efficiency [2,3]. On the other hand, it is know the efficiency of host catalase and selenocysteine-containing glutathione peroxidases for hydroperoxide detoxifying [4,5]. In members of the family Trypanosomatidae, peroxide metabolism mainly involves trypanothione [*N*1,*N*8-bis (glutathionyl)-spermidine, ($T(SH)_2$)], a glutathionyl derivative of spermidine. In these organisms it is present a system able to catalyze the $T(SH)_2$-dependent hydroperoxide removal, which involves three distinctive oxidoreductases: *(i)* trypanothione reductase (TR), homologous to glutathione reductase [6–9]; *(ii)* a thioredoxin-related protein called tryparedoxin (TXN); *(iii)* tryparedoxin peroxidases (TXNPx); and (*iv*) glutathione peroxidase-type proteins [2,10–15]. It has been proposed that these redox components operate in the parasite instead of the host specific thioredoxin (TRX)-thioredoxin reductase (TRXR) system [6]. In fact, TRXR is absent in trypanosomatids [16–18].

After more than 100 years from the discovery of Chagas' disease, the only drugs with a proven efficacy against the infection are nifurtimox (Nfx) and benznidazole (Bnz) (nitrofuran and nitroimidazole, respectively). These two drugs have been used to treat Chagas' disease for over 40 years; even when they can cause not only a large variety of unwanted side effects (sometimes forcing the patient to abandon the treatment), but also presents a variable

* Corresponding author. Instituto de Agrobiotecnología del Litoral (IAL), Centro Científico Tecnológico Santa Fe (CCT), Colectora Ruta Nac. Nº168, Paraje el Pozo s/n, 3000 Santa Fe, Argentina.
*E-mail address:* saguerrero@santafe-conicet.gov.ar (S.A. Guerrero).

http://dx.doi.org/10.1016/j.ejmech.2016.10.055
0223-5234/

therapeutic efficacy and high cost [19–22]. In this framework, the characterization of relevant biochemical targets in *T. cruzi* and rational design of specific inhibitors constitute critical issues to develop new chemotherapeutic drugs, more effective and less toxic than Bnz or Nfx. The action of Nfx through a redox cycling mechanism has been questioned [22–24]. In fact, this drug require bioactivation trough a reduction step that is catalyzed by specific nitroreductases of the parasite (*Tcr*NTR) [25–27]. Type I *Tcr*NTR, mediates a 2 electrons reduction of nitroaromatic compounds to yield aromatic amines able to interact with DNA and other essential macromolecules, thus affecting cellular functionality. Besides, a type II *Tcr*NTR functions catalyzing a 1 electron reduction of nitro compounds to render nitro radical anions [26,28]. As it emerges from previous works [29], TR is a metabolic bottleneck of interest for rational design of new inhibitors with potential trypanocide activity (Fig. 1). The enzyme from *T. cruzi* (*Tcr*TR), which has been well characterized, is closely related to human glutathione reductase (hGR) [8,9]. Both enzymes have a homodimeric structure (subunits molecular mass of ~52 kDa) and catalyze reduction equivalents transference from NADPH to their respective disulfide substrates through FAD and a redox active cysteine disulfide. Although *Tcr*TR has 40% sequence identity with hGR [8,9], the former uses $T(SH)_2$ but not glutathione (GSH) as a substrate. The three dimensional structure of *Tcr*TR [30–32] has been solved, which is of great relevance for molecular docking studies [33–36]. A recent review from Maya and co-workers [37] resume all compounds that were designed based in *Tcr*TR 3D structure, most of them without a trypanocide improved effect.

Herein, the synthesis and characterization of a family of new synthetic compounds derivatives from 5-nitro-2-furoic acid (5-NFA) is presented, being their potential as trypanocide drugs evaluated. All compounds were rationally designed based in our search of hypothetical compounds capable of interfering with *Tcr*TR in the transference of reduction equivalents from NADPH to generate $T(SH)_2$ (Fig. 1). Synthetic compounds were designed containing a nitrofuran structure, amide bonds with linear and cyclic amines, diamines and aromatic amines, according to an analogy with Nfx and Bnz. In general, synthetic structures were able to delocalize reduction electrons in the oxidoreductases cascade above described. For the amide bond formation we have developed different synthetic methodologies from the 5-NFA directly or by transformation of its derivative acid chloride, Fig. 2.

## 2. Results and discussion

### 2.1. Rational design of TcrTR inhibitors

Currently available literature clearly points out that TR is a key enzyme for transferring reducing equivalents from NADPH to various cellular acceptors, through $T(SH)_2$ (Fig. 1). It was thought in designing compounds that could interfere in such a flow of reducing equivalents, thus disturbing the normal performance of the oxidoreductases cascade. Accordingly, different derivatives of the 5-NFA were synthesized by substituting the carboxylic group in position 2 of 5-NFA by an amide group with varied amines to obtain synthetic species able to trap reducing equivalents. By combination of regions of functional groups with progressive degree of complexity, a series of secondary and tertiary amides structurally related to Nfx and Bnz (named compounds **1**–**13**, see Fig. 2**)** were synthesized and also optimized with good yields. All these compounds were identified by NMR spectroscopy (analyses detailed in Materials and Methods and Supplemental Material) for further bioassays. The results obtained after bioactivity and computational docking studies support the design of appropriate chemical analogues after combining molecular structures of compounds with recognized trypanocidal activity.

### 2.2. Antiparasitic activity of 5-NFA derivatives on T. cruzi epimastigotes

*In vitro* assays testing antiproliferative effect of the new compounds were performed on *T. cruzi* Dm28c epimastigotes. Axenic

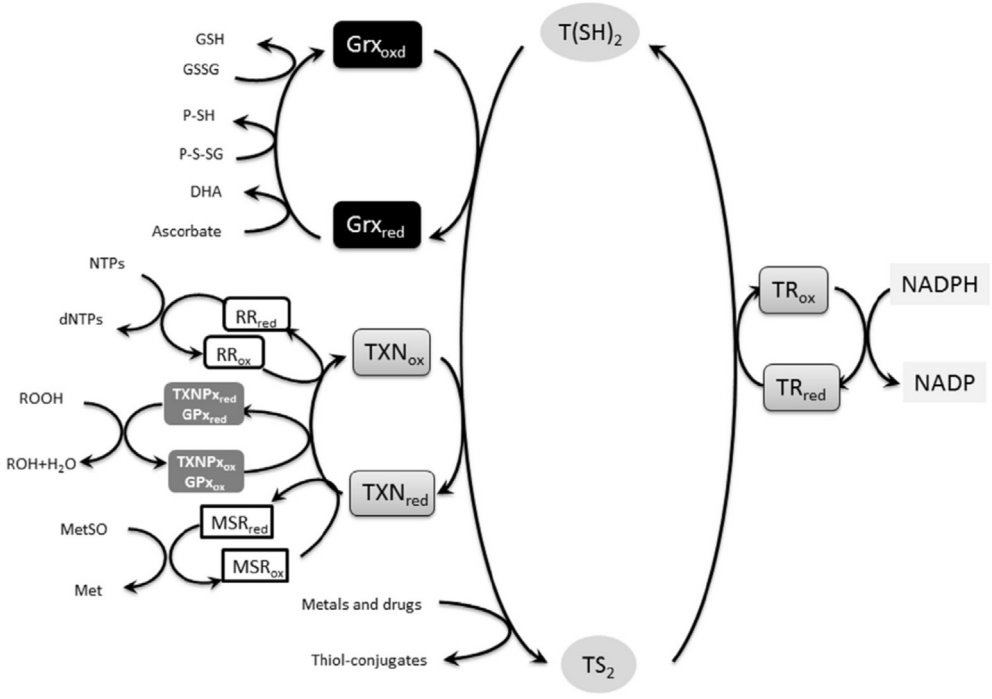


**Fig. 1.** Trypanothione dependent redox metabolism. TRox, oxidized trypanothione reductase; TRred, reduced trypanothione reductase. In this system, reduced trypanothione can transfers reduction equivalents to several metabolic pathways [29].

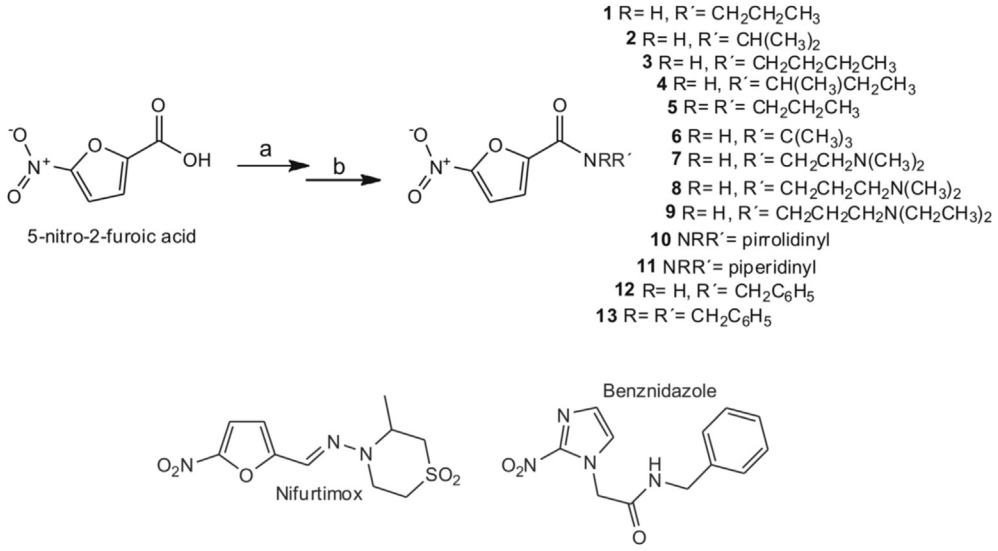


**Fig. 2.** Synthesis of amides **1**–**13**: a) 5-NFA (0.64 mmol), $SOCl_2$ (3 mL), reflux 1 h; b) acetone (2.2 mL), selected amine (0.86 mmol) in pyridine (0.5 mL), RT. 20 h.

cultures of the parasite were incubated with increasing amounts of each compound to determine the respective 50% inhibitory concentration ($IC_{50}$) of 48 h of cells growth. The results indicate that all 5-NFA derivatives evaluated showed antiparasitic activity, each one with different potency (Table 1). Conversely, 5-NFA exhibited no effect on *T. cruzi* cultures (Fig. 3). Nfx, one referent drug for the treatment of Chagas's disease [38], having a low $IC_{50}$ (4.0 μM), was used as experimental control. Among all 5-NFA derivatives evaluated, compounds **1, 2, 8, 12** and **13** displayed activity against epimastigotes with $IC_{50}$ values between 1 and 19 μM, causing morphological alterations in the parasite (Fig. 3). In order to analyze the toxicity of all synthetic compounds on mammalian cells, the cytotoxicity on HeLa cells of those derivatives with low $IC_{50}$ values for *T. cruzi* epimastigotes (less than 25 μM) were determined. Eight compounds were studied in their toxic activity toward HeLa cells. Mammalian cells were treated with different inhibitor concentrations, and after 24 h living cells were visualized with crystal violet staining. HeLa cells revealed generally higher $EC_{50}$ values, which resulted in selectivity indexes of 4 or higher (Table 1). Interestingly, compound **13** exhibited the highest value of both potency against *T. cruzi* cells and selectivity index in comparison with the other derivatives. The behavior of compound **13** is similar to that identified for Nfx, which might indicate that both compounds could follow the same action mechanism. Some interesting structure–activity relationships for compound **13** emerged after compilation of the results (Table 1). A comparison of the series of compounds derived from 5-NFA indicates that the introduction of aliphatic tertiary amines or benzylamide moieties apparently enhances the trypanocide activity.

### 2.3. Inhibition of TcrTR activity by 5-NFA derivatives

TR activity was not affected by 5-NFA (Fig. 4); however, 5-NFA derivatives (**8**, **12**, and **13**) showed an inhibitory effect on TR activity, following a pattern of linear reversible uncompetitive inhibition regarding $TS_2$ substrate (Fig. 4 A). Thus, the inhibition takes place and according to the following mechanism:

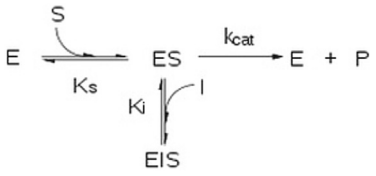


**Table 1**
*In vitro* enzyme inhibition and cellular toxicity activity of nitro-derivate compounds.

| Drug | *Tc*TR inhibition (regarding to $TS_2$)[a] | *T. cruzi* growth inhibition | HeLa cells toxicity | Selectivity index |
|---|---|---|---|---|
| | *Ki* (μM) | $IC_{50}$ (μM) | $EC_{50}$ (μM) | HeLa/*T. cruzi* |
| **1** | 336 (U) | 17 ± 3 | 150 ± 22 | 8.8 |
| **2** | 414 (U) | 18 ± 2 | 211 ± 19 | 11.7 |
| **3** | 315 (U) | 26 ± 3 | 152 ± 23 | 5.8 |
| **4** | 1180 (U) | 23 ± 4 | 165 ± 18 | 7.2 |
| **5** | 183 (U) | 19.6 ± 0.8 | – | – |
| **6** | 313 (U) | 35 ± 5 | – | – |
| **7** | 136 (U) | 36 ± 3 | – | – |
| **8** | 118 (U) | 19 ± 3 | 74 ± 7 | 3.9 |
| **9** | 128 (U) | 25 ± 2 | 100 ± 6 | 4.0 |
| **10** | 187 (U) | 64 ± 11 | – | – |
| **11** | 282 (U) | 103 ± 25 | – | – |
| **12** | 61 (U) | 15 ± 2 | 123 ± 11 | 8.2 |
| **13** | 68 (U) | 1.1 ± 0.1 | 78 ± 9 | 70.1 |
| Nfx | 245 (U) | 4.0 ± 0.8 | 272 ± 70 | 68.0 |

(U) = classic reversible uncompetitive inhibition.
[a] At pH 7.5 and 30 °C.

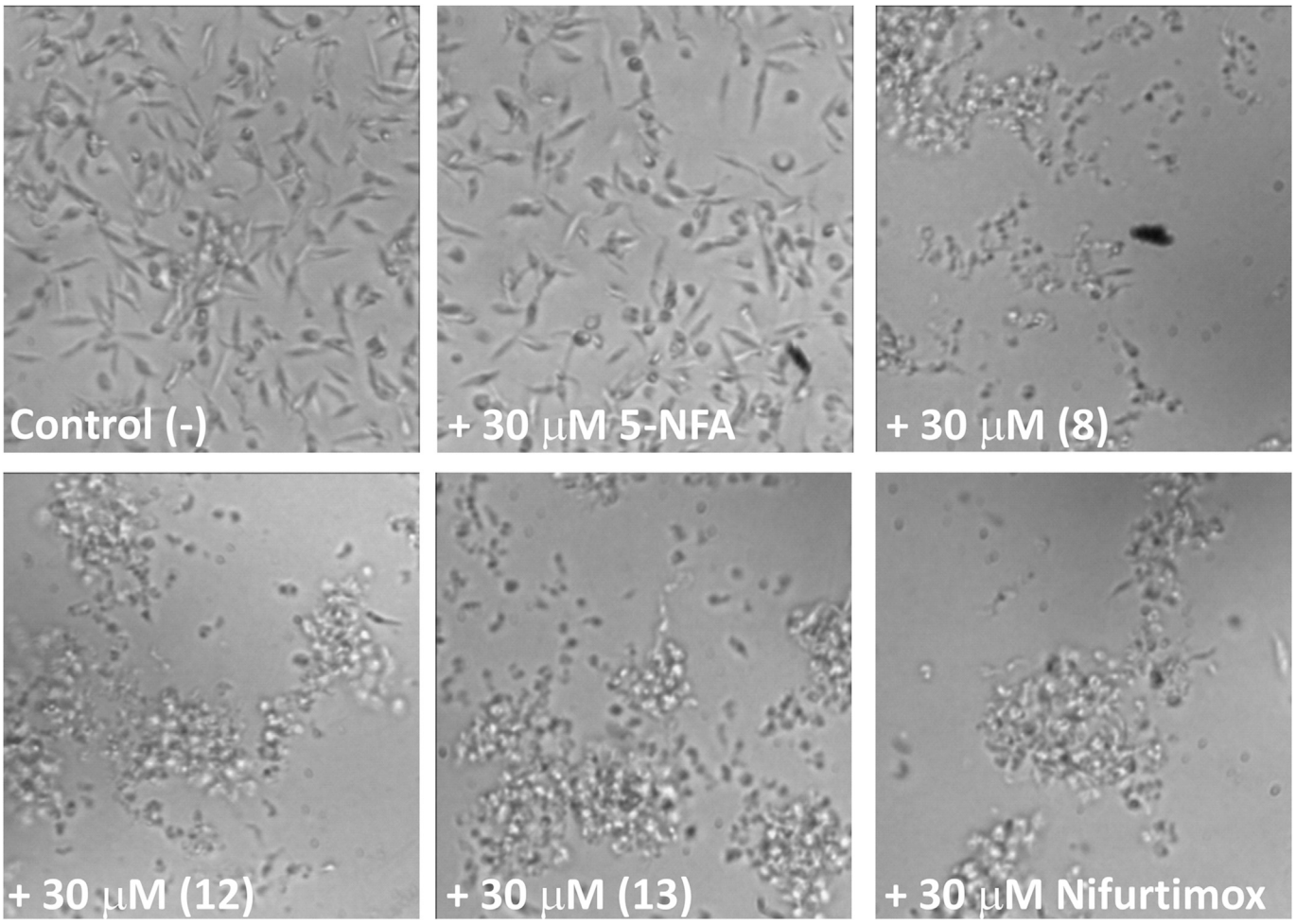


**Fig. 3.** Cytotoxic effect of 5-NFA derivatives on *T. cruzi* epimastigotes cultures. Suspensions of logarithmic-phase *T. cruzi* Dm28c epimastigotes ($10^6$ cell/ml) were incubated for 48 h in LIT-supplement medium in absence or in presence of the 5-NFA derivatives were added.

Where *K*s is the dissociation constant for enzyme–substrate complex (ES), $k_{cat}$ is the catalytic constant and *K*i is the dissociation constant for enzyme–substrate-inhibitor complex (EIS). Values of *K*i and inhibition type were calculated as detailed in Table 1, and the behavior of 5-NFA derivatives as inhibitors of TR was compared with previous reports for other synthetic uncompetitive inhibitors, such as 1,4-naphthoquinone derivatives [39]. Interestingly, the results indicate that Nfx exhibited a relatively low inhibitory effect on the enzyme, but many of the compounds we synthesized from 5-NFA exhibited a valuable inhibitory effect (Table 1). The lack of correlation between TR inhibition and cytotoxic effect on *T. cruzi* epimastigotes for several 5-NFA derivatives and Nfx, suggest that the trypanocide effect could be not due only to the interaction with TR, but also to other enzymes. However, the synthetic inhibitor **13**, between all the compounds studied herein, fitted the best correlation between inhibitory effect on the enzyme activity (low *K*i value) and high potency against *T. cruzi* cells with respect to other derivatives.

### *2.4. Computational docking studies of synthetic compounds against TcrTR*

An energetic evaluation of binding affinity was first performed, followed by a structural analysis of the results. Such affinities for the best poses obtained for each of the docking simulation are shown in Table 2 for interactions with *Tcr*TR. For the structure of the enzyme interacting with trypanothione, Nfx and compound **12** have the best affinity for the protein (with similar binding energies) and following them are the **13** and **8** molecules. Structurally, the four molecules bind at the same position on the *T. cruzi* enzyme structure with trypanothione at region R1 (Fig. 5), indicating that all the molecules are located on the $TS_2$ moiety. At region R2, the four molecules interact directly with the $TS_2$, as in R1, but there are two distinctive regions of interaction located close to both extremes of the substrate structure (Fig. 6). This different behavior of the molecules on both regions could be related to the respective changes in conformation observed for the $TS_2$ molecule on each region (R1 and R2). The carboxylic group of the trypanothione on region R2 is pointing away from the binding site (Fig. 7) and because of that some of the molecules interact directly with this group (**12** and Nfx). We observed that in the 3D structure of *Tcr*TR (without trypanothione), the four molecules interact with the protein with acceptable predicted score for their binding affinity, but since they are smaller, they interacts only with the part of the cavities that is usually occupied by the terminal portion (the glutamic acid residue) of the $TS_2$ (when it is bound to *Tcr*TR).

## 3. Conclusions

Nfx, is thought to affect the viability of trypanosomes by the formation of both reactive oxygen species and highly toxic

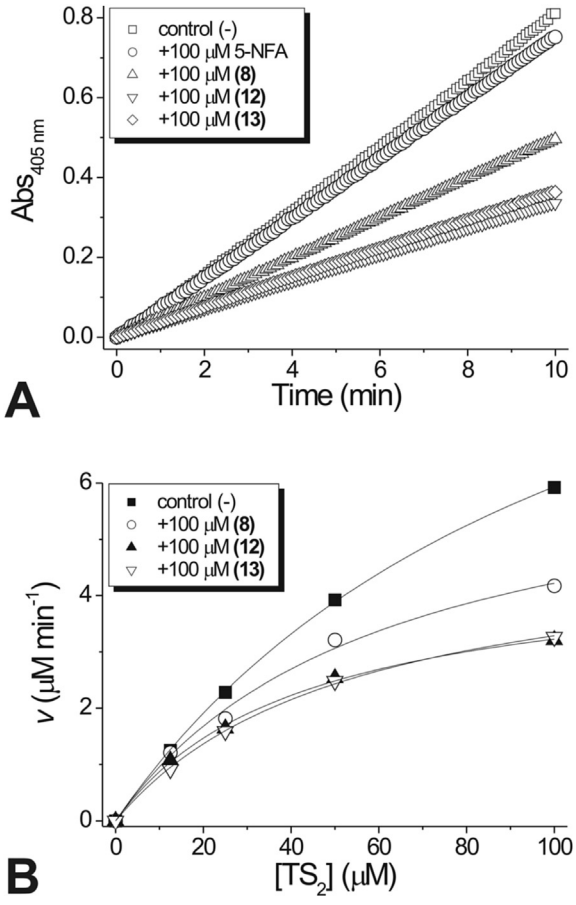


**Fig. 4.** Inhibition of trypanothione reductase activity by 5-NFA derivatives. A) Time-dependent inhibition of *Tcr*TR by nitro-derivative compounds. Assays were carried out at 30 °C, pH 7.5 and the reaction mixture included 4 nM *Tcr*TR, 0.2 mM NADPH, 0.5 mM DTNB and 5 μM $TS_2$ and 100 μM of 5-NFA, **8**, **12 or 13**. B) Plot of initial rate ($v$) from progress curves as a function of $TS_2$ concentration.

**Table 2**
Binding energies in Kcal/mol for the interactions of each molecule with the trypanothione reductase from *Trypanosoma cruzi*. The calculations were done with AutoDock Vina.

| *T. cruzi* | With Trypanothione | | Without Trypanothione | |
|---|---|---|---|---|
| | R1 | R2 | R1 | R2 |
| **8** | −6.1 | −6.0 | −6.0 | −6.1 |
| **12** | −6.9 | −6.7 | −7.3 | −7.0 |
| Nfx | −6.7 | −7.2 | −7.3 | −7.0 |
| **13** | −6.4 | −6.6 | −7.8 | −7.3 |

hydroxylamine derivatives. The treatment of American Trypanosomiasis with Nfx or Bnz has variable efficacy and severe side effects. It is clear the relevance that nowadays represents the evaluation of new chemotherapeutic agents in order to improve efficacy of antichagasic therapy. In this work, a series of 5-NFA analogues were rationally designed and synthesized. Their trypanocidal activity against epimastigote forms of *T. cruzi* was tested. The toxic effects of synthetic compounds were tested on human HeLa cells. Between all the compounds synthesized, three of thirteen could overcome Nfx in their trypanocidal activity. Moreover, compound **13** was able to improve it (IC50 value much lower than Nfx). Compound **13** showed a selective index of 70 after evaluation the toxicity against HeLa cells and an $IC_{50}$ four-fold lower than that determined for Nfx. Its activity to interfere in the flux of reducing equivalents from NADPH to oxidizing substrates (using reduced trypanothione as the major pivotal thiol) was tested. Hence, trypanothione reductase was selected as a critical target for this study, analyzing in vitro the enzyme inhibition by Nfx and compounds **8**, **12** and **13**. All compounds showed a better inhibition parameter than Nfx. In all inhibition reaction the mechanism for enzyme inhibition followed an uncompetitive pattern. The introduction of aliphatic tertiary amines or benzylamide substituents improved the inhibitory potency of the series of 5-NFA derivatives, being the ability of such compounds to inhibit *Tcr*TR activity and parasite growth dependent exclusively on the structure and nature of their substituents. Molecular docking analysis enabled us to study the type of interaction between *Tcr*TR and four of the synthetic *inhibitors* (Nfx, **8**, **12** and **13**). First, and very important, docking assays showed that Nfx can be able of binding to *Tcr*TR. That could be another possibility of the drug to affect the viability of the parasite in addition to those reported previously and related to nitroreductases activities. In the same way, molecular docking shows that in *T. cruzi* the molecules of inhibitors can bind directly to the complex *Tcr*TR-trypanothione, which strongly supports our previous experimental findings of a pattern of linear reversible uncompetitive inhibition. Fig. 6 shows the analog **13** (which have rotation free due to methylene of the benzyl group), with the phenyl groups located in parallel with a probable pi interaction that it is not possible in the compound **12**. Conversely, the incorporation of an N-amide inserted into a ring such as the analogues **10** and **11**, produces a structural rigidity that could cause the loss of bioactivity in respect with **13**.

Current results about properties of compound **13** for affecting the viability of *T. cruzi* epimastimote cells, its activity as uncompetitive inhibitor of *Tcr*TR and its evidenced capability to interact with the complex *Tcr*TR-$TS_2$ highlight this synthetic molecule as relevant to develop new and effective drugs. Further studies are necessary to reach such an advance in the fight against diseases caused by trypanosomatids. Moreover, TR is an enzyme conserved in all trypanosomatids, so our results could be of relevance for extending this study to the development of inhibitors for TR from *Leishmania* spp. or *Trypanosoma brucei* spp.

## 4. Materials and methods

### 4.1. Materials

Bacteriological media. Trypanothione disulfide ($TS_2$) was acquired from Bachem. All other reagents and chemicals were of the highest quality commercially available from Sigma Aldrich, Merck, Invitrogen and Promega.

### 4.2. Trypanosoma cruzi cultures

*T. cruzi Dm*28c epimastigote cells were cultivated axenically at 28 °C in LIT media supplemented with 10% (w/v) bovine fetal serum and 20 μg $ml^{-1}$ hemin, as previously reported [40].

### 4.3. Chemistry, general

All reagents and solvents were purchased in Sigma-Aldrich and Sintorgan and were used directly as purchased or purified according to standard procedures. All reactions involving air or moisture-sensitive materials were carried out under nitrogen atmosphere. All reaction products were purified by flash chromatography which was performed with 300–400 mesh silicagel under slight nitrogen pressure, with increasing gradients of solvent mixtures. IR spectra were recorded with a *Shimadzu*, *Prestige 21* Model

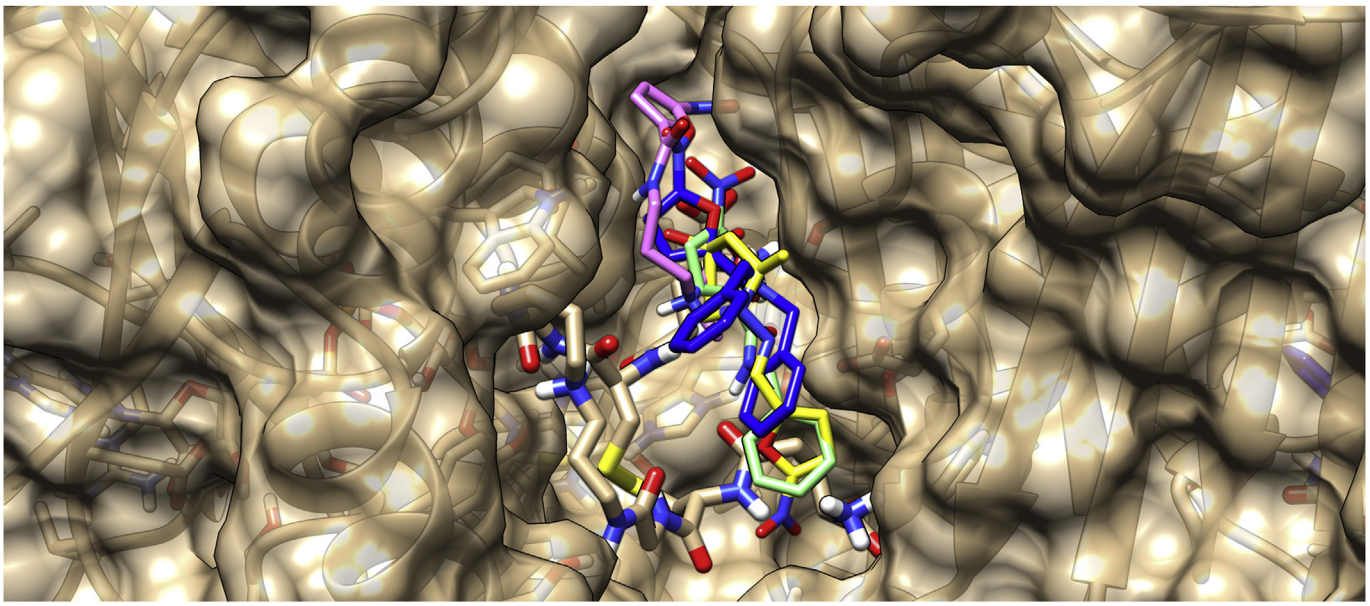

**Fig. 5.** Binding poses of the four molecules at the region R1 of *Tcr*TR (with $TS_2$). Color code: **8** (pink), **12** (green), Nfx (yellow) and **13** (blue). (For interpretation of the references to colour in this figure legend, the reader is referred to the web version of this article.)

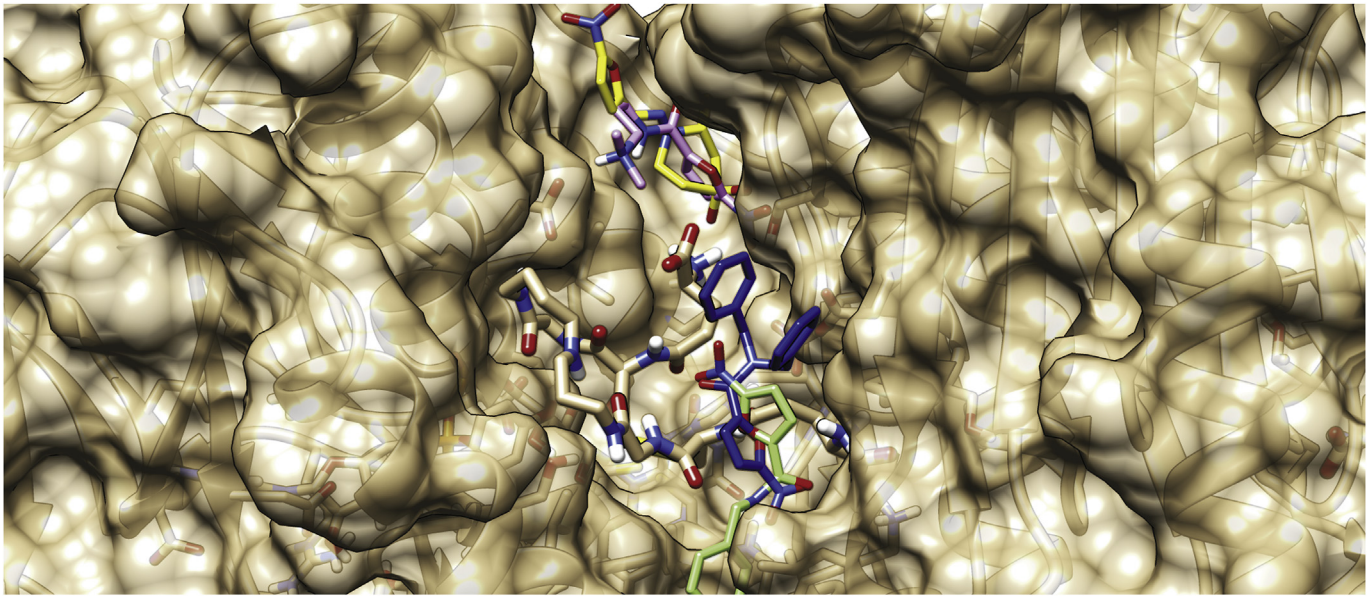

**Fig. 6.** Binding poses of the four molecules at the region R2 of *Tcr*TR (with $TS_2$). Color code: **8** (pink), **12** (green), Nfx (yellow) and **13** (blue). (For interpretation of the references to colour in this figure legend, the reader is referred to the web version of this article.)

spectrophotometer, with samples as liquid films in NaCl for oils and KBr disks for solids. NMR experiments were run in $CDCl_3$ at 300.13 MHz for $^1H$ NMR and at 75.4 MHz for $^{13}C$ NMR with a *Bruker Avance-300 MHz* NMR spectrometer and the corresponding solvent as internal reference standard. High-resolution mass spectrometry was carried out with a *LC-QTOf Bruker MicroTOF QII*. GC-MS spectra were recorded with a *Shimadzu* QP-2010 plus spectrometer (see supplemental information).

### 4.4. Synthesis and characterization of compounds

A stirred mixture of 5-nitrofuroic acid (5-NFA 100 mg; 0.64 mmol) and $SOCl_2$ (3 mL) was refluxed in a silicone bath for 1 h until gas evolution stops. The reaction mixture was left to take room temperature and, with the addition of anhydrous toluene (1 mL), the excess of $SOCl_2$ was evaporated *in vacuo*. Then, a solution of selected amine (0.86 mmol in 0.5 mL of anhydrous pyridine) was dropwise added to the acid chloride (obtained as oil) dissolved in anhydrous acetone (2.2 mL) and the mixture was maintained at room temperature for 18–22 h. The reaction mixture was diluted with EtOH, concentrated *in vacuo* and dried to give a residue which was purified by chromatographic column. Yield: 62–95%.

#### 4.4.1. 5-Nitro-2-furoic acid (5-nitrofuran-2-carboxilic acid, 5-NFA)

commercial starting material: $^1H$ NMR ($CDCl_3$) $\delta$ (ppm): 7.31 (d, 1H, $J = 3.7$ Hz, HC═CC═O), 7.23 (d, 1H, $J = 3.8$ Hz, HC═C-$NO_2$), 7.42

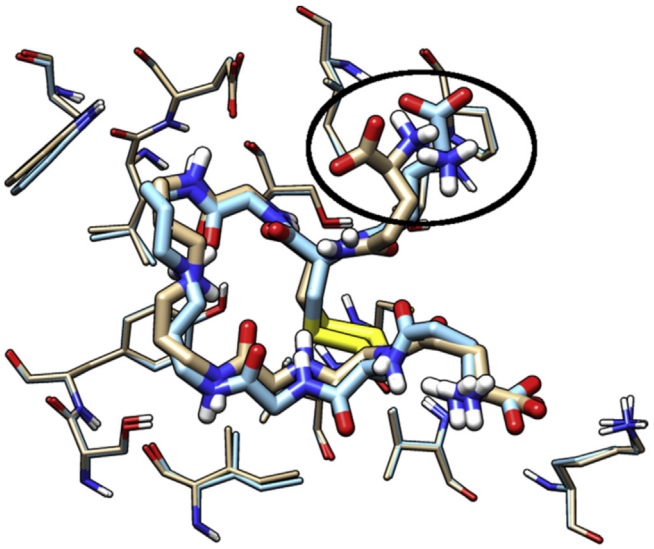

**Fig. 7.** Superposition of the conformations of the $TS_2$ molecule in regions R1 and R2 in *Tcr*TR. The circle shows the most important change between both.

(br s, 1H, COOH).

*4.4.2. 5-Nitro-furan-2-carboxylic acid propylamide* ***(1)***

Two chromatographic columns with solvent mixture ($CH_2Cl_2$/MeOH, 99:1). Yield: 93 mg, 0.47 mmol, 73%. Crystalline, m.p. = 97.1–99.3 °C. IR (film) $\nu$ ($cm^{-1}$): 3304 (N-H), 3119 (CH furane), 2967, 2875 (CH alkane), 1681 (C=O), 1584, 1485, 1385 (C=C furane), 1556 (C-N), 1352 ($NO_2$), 1288 (C-N), 1016 (C-O). $^1$H NMR ($CDCl_3$) $\delta$ (ppm): 7.35 (d, 1H, $J$ = 3.8 Hz, H-3), 7.23 (d, 1H, $J$ = 3.8 Hz, H-4), 6.68 (br s, 1H, NH), 3.41 (c, 2H, $J$ = 6.3 Hz, NHC$H_2$-), 1.65 (dt, 2H, $J$ = 7.3, 14.8 Hz, $NHCH_2CH_2CH_3$), 0.97 (t, 3H, $J$ = 7.4 Hz, $NHCH_2CH_2CH_3$). $^{13}$C NMR ($CDCl_3$) $\delta$ (ppm): 156.3 (C=O amide), 151.3 (C-5), 148.3 (C-2), 115.7 (C-4), 112.5 (C-3), 41.3 ($NHCH_2$-), 22.7 ($NHCH_2CH_2CH_3$), 11.3 ($NHCH_2CH_2CH_3$). EIHRMS calculated mass for $C_8H_{10}N_2O_4Na$ ($M + Na^+$) = 221.05328; found 221.05294.

*4.4.3. 5-Nitro-furan-2-carboxylic acid isopropylamide* ***(2)***

Solvent mixture for purification ($CH_2Cl_2$/MeOH, 99:1). Yield: 77 mg, 0.40 mmol, 63%. White solid, m.p. = 117.7–118.1 °C. IR (film) $\nu$ ($cm^{-1}$): 3294 (N-H), 3136 (CH furane), 2976, 2875 (CH), 1651 (C=O), 1584, 1557, 1485, 1386 (C=C furane), 1352 ($NO_2$), 1279 (C-N amide), 1171, 1146 (*gem*-$CH_3$). $^1$H NMR ($CDCl_3$) $\delta$ (ppm): 6.40 (br s, 1H, NH), 7.35 (d, 1H, $J$ = 3.8 Hz, H-3), 7.23 (d, 1H, $J$ = 3.8 Hz, H-4), 6.40 (br s, 1H, NH), 4.26 (m, 1H, $J$ = 6.7 Hz, $(CH_3)_2CH$N-), 1.28 (d, 6H, $J$ = 6.6 hz, $CH_3$). $^{13}$C NMR ($CDCl_3$) $\delta$ (ppm): 155.4 (C-5), 151.2 (C=O), 148.4 (C-2), 115.7 (C-4), 112.5 (C-3), 42.0 ($(CH_3)_2CH$N-), 22.6 ($(CH_3)_2$CHN). EIHRMS calculated mass for $C_8H_{10}N_2NaO_4$ ($M + Na^+$) = 221.05328; found 221.05374

*4.4.4. 5-Nitro-furan-2-carboxylic acid butylamide* ***(3)***

Solvent mixture for purification ($CH_2Cl_2$/MeOH, 99:1). Yield: 89 mg, 0.42 mmol, 66%. Ambar oil. IR (film) $\nu$ ($cm^{-1}$): 3304 (N-H), 3138 (CH alkane), 2959, 2872 (CH), 1651 (C=O amide), 1584, 1485, 1390 (C=C), 1556, 1352 ($NO_2$), 1286 (C-N amide), 1016 (C-O). $^1$H NMR ($CDCl_3$) $\delta$ (ppm): 7.35 (m, 1H, H-3), 7.24 (d, 1H, $J$ = 3.6 Hz, H-4), 6.65 (br s, 1H, NH), 3.45 (c, 2H, $J$ = 6.6 Hz, NHC$H_2$-), 1.61 (q, 2H, $J$ = 7.3 Hz,$CH_2CH_2CH_2$), 1.39 (m, 2H, $J$ = 7.1 Hz, C$H_2CH_3$), 0.95 (t, 3H, $J$ = 7.3 Hz, $CH_2CH_3$). $^{13}$C NMR ($CDCl_3$) $\delta$ (ppm): 156.3 (C=O amide), 151.1 (C-5), 148.3 (C-2), 115.8 (C-4), 112.5 (C-3), 39.4 ($NHCH_2CH_2CH_2$), 31.5 ($NHCH_2CH_2CH_2$), 20.0 ($CH_2CH_2CH_2$), 13.7 ($CH_2CH_3$). EIHRMS calculated mass for $C_9H_{12}N_2O_4Na$ ($M + Na^+$) = 235.06893; found 235.06967.

*4.4.5. 5-Nitro-furan-2-carboxylic acid sec-butylamide* ***(4)***

Solvent mixture for purification ($CH_2Cl_2$). Yield: 91 mg, 0.43 mmol, 68%. Yellow oil. IR (film) $\nu$ ($cm^{-1}$): 3123 (CH furane), 2968 (CH), 1653 (C=O), 1553, 1485 (C=C furane), 1526, 1352 (NO), 1387 (CN), 1287 (CN), 1016 (CO furane), 810 (CN). $^1$H NMR ($CDCl_3$) $\delta$ (ppm): 7.34 (d, 1H, $J$ = 7.7 Hz, H-3), 7.22 (d, 1H, $J$ = 7.9 Hz, H-4), 6.39 (br s, 1H, NH), 4.08 (m, 1H, CH), 1.59 (m, 2H, $J$ = 7.3 Hz, C$H_2CH_3$), 1.24 (d, 3H, $J$ = 6.6 Hz, CHC$H_3$), 0.94 (t, 3H, $J$ = 7.4 Hz, $CH_2CH_3$). $^{13}$C NMR ($CDCl_3$) $\delta$ (ppm): 155.7 (C=O), 151.1 (C-5), 148.4 (C-2), 115.7 (C-4), 112.6 (C-3), 47.3 (CH), 29.5 (C$H_2CH_3$), 20.3 ($CH_3$), 10.4 ($CH_2CH_3$). EIHRMS calculated mass for $C_9H_{12}N_2NaO_4$($M + Na^+$) = 235.06893, found 235.06975.

*4.4.6. 5-Nitro-furan-2-carboxylic acid-dipropyl-amide* ***(5)***

Solvent mixture for purification (Hexane/$CH_2Cl_2$, 30:70). Yield: 129 mg, 0.54 mmol, 85%. Yellow oil, IR (film) $\nu$ ($cm^{-1}$): 3132 (CH furane), 2966, 2874 (CH), 1636 (C=O), 1578, 1423 (C=C furane), 1381 (CN), 1350 (NO), 1254 (CN), 1018 (CO furane), 814 (CN nitro). $^1$H NMR ($CDCl_3$) $\delta$ (ppm): 7.33 (d, 1H, $J$ = 3.8 Hz, H-3), 7.20 (d, 1H, $J$ = 3.8 Hz, H-4), 3.53 (t, 2H, $J$ = 7.8 Hz, $NCH_2$), 3.43 (t, 2H, $J$ = 7.7 Hz, $NCH_2$), 1.74 (m, 2H, C$H_2CH_3$), 1.66 (m, 2H, C$H_2CH_3$), 0.97 (m, 3H, $CH_2CH_3$). $^{13}$C NMR ($CDCl_3$) $\delta$ (ppm): 157.5 (C=O), 151.1 (C-5), 149.3 (C-2), 118.0 (C-4), 111.7 (C-3), 50.5, 49.3 ($NCH_2$), 22.9, 20.6 ($CH_2CH_3$), 11.3, 10.9 ($CH_3$). EIHRMS calculated mass for $C_{11}H_{16}N_2NaO_4$ ($M + Na^+$) = 263.10078, found 263.10023.

*4.4.7. 5-Nitro-furan-2-carboxylic acid tert-butylamide* ***(6)***

Solvent mixture for purification (Hexane/$CH_2Cl_2$, 30:70). Yield: 102 mg, 0.48 mmol, 75%. Yellow solid, m.p. = 103.5–104.4 °C. IR (film) $\nu$ ($cm^{-1}$): 3317 (NH amide), 3136 (C-H furane), 2970, 2873 (CH), 1678 (C=O), 1589, 1485, 1389 (C=C furane), 1550, 1354 ($NO_2$), 1292 (CN), 1219 (*t*-butyl), 813 (CN nitro). $^1$H NMR ($CDCl_3$) $\delta$ (ppm): 7.33 (d, 1H, $J$ = 3.8 Hz, H-3), 7.18 (d, 1H, $J$ = 3.8 Hz, H-4), 6.35 (br s, 1H, NH), 1.47 (s, 9H, $CH_3$). $^{13}$C NMR ($CDCl_3$) $\delta$ (ppm): 155.5 (C-5), 150.9 (C=O), 148.8 (C-2), 115.4 (C-4), 112.6 (C-3), 52.4 (C$(CH_3)_3$), 28.7 ($CH_3$). EIHRMS calculated mass for $C_9H_{12}N_2NaO_4$ ($M + Na^+$) = 235.0695, found 235.06902.

*4.4.8. 5-Nitro-furan-2-carboxylic acid (2-dimethylamino-ethyl)-amide* ***(7)***

Solvent mixture for purification ($CH_2Cl_2$/MeOH, 90:10). Yield: 88 mg, 0.39 mmol, 62%. Yellow oil. IR (film) $\nu$ ($cm^{-1}$): 3394 (CH furane), 3120 (CH), 2920, 2780 (C-H), 1660 (C=O), 1581, 1531, 1481 (C=C furane), 1555, 1354 (N-O), 1389, 1290 (C-N amine), 1022 (CO furane), 814 (CN nitro). $^1$H NMR ($CDCl_3$) $\delta$ (ppm): 7.66 (br s, 1H, $J$ = 5.5 Hz, N-H), 7.38 (d, 1H, $J$ = 3.9 Hz, H-3), 7.25 (d, 1H, $J$ = 3.9 Hz, H-4), 3.54 (c, 2H, $J$ = 5.5 Hz, $NCH_2$), 2.56 (t, 2H, $J$ = 6.2 Hz, $NCH_2$ C$H_2$), 2.31 (s, 6H, $NCH_3$). $^{13}$C NMR ($CDCl_3$) $\delta$ (ppm): 156.4 (C=O), 151.3 (C-5), 148.3 (C-2), 115.7 (C-4), 112.4 (C-3), 57.5 ($NCH_2$), 45.1 ($CH_3$), 36.8 ($NHCH_3$). EIHRMS calculated mass for $C_9H_{13}N_2NaO_4$ ($M + Na^+$) = 250.0804, found 250.07983.

*4.4.9. 5-Nitro-furan-2-carboxylic acid (3-dimethylamino-propyl)-amide* ***(8)***

Solvent mixture for purification ($CH_2Cl_2$/MeOH, 94:6). Yield: 90 mg, 0.41 mmol, 64%. White solid, m.p. = 131.5–135.2 °C. IR (film) $\nu$ ($cm^{-1}$): 3300 (N-H), 3125 (CH furane), 2949, 2922, 2860, 2822, 2781 (C-H), 1661 (C=O), 1582 (C=C), 1531 (C=C furane), 1552, 1352 ($NO_2$), 1290 (CN), 1016 (C-O), 968, 812.$^1$H NMR ($CDCl_3$) $\delta$ (ppm): 9.59 (br s, 1H, NH), 7.33 (d, 1H, $J$ = 3.8 Hz, H-3), 7.21 (d, 1H, $J$ = 3.7 Hz, H-4), 3.56 (dd, 2H, $J$ = 5.4 Hz, $(CH_3)_2NCH_2$-), 2.62 (t, 2H, $J$ = 5.9 Hz, $NHCH_2CH_2CH_2$), 2.41 (s, 6H, *gem*-$CH_3$), 1.80 (q, 2H, $J$ = 5.8 Hz, $NHCH_2CH_2CH_2$). $^{13}$C NMR ($CDCl_3$) $\delta$ (ppm): 156.3 (C-5),

151.2 (C=O), 156.3 (C-5), 148.9 (C-2), 115.0 (C-4), 112.3 (C-3), 58.8 ($NHCH_2CH_2CH_2$), 44.7 (*gem*-$CH_3$), 40.1 ($CH_2CH_2CH_2N(CH_3)_2$), 24.4 ($NHCH_2CH_2CH_2$). EIHRMS calculated mass for $C_{10}H_{16}N_3O_4$ ($M + H^+$) = 242.1135; found 242.1136.

#### 4.4.10. 5-Nitro-furan-2-carboxylic acid (3-diethylamino-propyl)-amide **(9)**

Solvent mixture for purification ($CH_2Cl_2$/MeOH, 96:4). Yield: 164 mg, 0.61 mmol, 95%. Ambar oil. IR (film) $\nu$ ($cm^{-1}$): 3279 (N-H), 3140 (CH furane), 2970, 2940, 2816 (CH), 1666 (C=O), 1578, 1555, 1350 (NO nitro), 1535, 1481 (C=C furane), 1288 (CN amide), 1018 (CO furane), 814 (C-N nitro group). $^1$H NMR ($CDCl_3$) $\delta$ (ppm): 9.67 (br s, 1H, NH), 7.30 (d, 1H, $J$ = 3.8 Hz, H-3), 7.20 (d, 1H, $J$ = 3.8 Hz, H-4), 3.51 (t, 2H, $J$ = 5.4 Hz, $NHCH_2$-), 2.66 (m, 4H, $J$ = 7.0 Hz, $Et_2NCH_2CH_2CH_2$, $NCH_2CH_3$), 1.76 (q, 2H, $J$ = 6.0 Hz, $NHCH_2CH_2CH_2$), 1.07 (t, 6H, $J$ = 7.1 Hz, $NHCH_2CH_3$). $^{13}$C NMR ($CDCl_3$) $\delta$ (ppm): 156.2 (C=O), 151.2 (C-5), 149.0 (C-2), 115.1 (C-4), 112.4 (C-3), 52.5 ($Et_2NCH_2CH_2CH_2$), 46.7 ($CH_2CH_3$), 40.4 ($NHCH_2CH_2CH_2$), 24.0 ($NHCH_2CH_2CH_2$), 10.9 ($CH_2CH_3$). EIHRMS: calculated mass for $C_{12}H_{20}N_3O_4$ ($M + H^+$) = 270.14483; found 270.14478.

#### 4.4.11. (5-Nitro-furan-2-yl)-pyrrolidin-1-yl-methanone **(10)**

Solvent mixture for purification ($CH_2Cl_2$/MeOH, 94:6). Yield: 105 mg, 0.50 mmol, 78%. Pale crystalls, m.p. = 160.8–161.8 °C. IR (film) $\nu$ ($cm^{-1}$): 3128 (CH furane), 2978 (CH), 1625 (C=O), 1582, 1493 (C=C furane), 1520, 1389 (CN), 1358 (NO), 1045 (CO furane), 814 (C-N). $^1$H NMR ($CDCl_3$) $\delta$ (ppm): 7.35 (d, 1H, $J$ = 3.8 Hz, H-3), 7.26 (d, 1H, $J$ = 3.8 Hz, H-4), 3.95 (t, 2H, $J$ = 6.8 Hz, $NCH_2$), 3.67 (t, 2H, $J$ = 6.8 Hz, $NCH_2$), 2.07 (m, 2H, $J$ = 6.8 Hz, -$CH_2$), 1.94 (m, 2H, $J$ = 6.8 Hz, -$CH_2$). $^{13}$C NMR ($CDCl_3$) $\delta$ (ppm): 155.7 (C=O), 151.4 (C-5), 149.3 (C-2), 117.6 (C-4), 111.8 (C-3), 47.7 ($NCH_2$), 47.6 ($NCH_2$), 26.5 ($NCH_2CH_2$), 23.6 ($NCH_2CH_2$). EIHRMS calculated mass for $C_9H_{11}N_2O_4$($M + H^+$) = 211.0713, found 211.0705

#### 4.4.12. (5-Nitro-furan-2-yl)-piperidin-1-yl-methanone **(11)**

Solvent mixture for purification ($CH_2Cl_2$/MeOH, 94:6). Yield: 121 mg, 0.54 mmol, 84%. White crystalls, m.p. = 96.5–96.7 °C. IR (film) $\nu$ ($cm^{-1}$): 3125 (CH furane), 2935 (CH), 1631 (C=O), 1578, 1435 (C=C furane), 1531, 1350 (NO), 1381 (CN), 1265 (CN), 1014 (CO furane), 810 (CN). $^1$H NMR ($CDCl_3$) $\delta$ (ppm): 7.33 (d, 1H, $J$ = 3.7 Hz, H-3), 7.09 (d, 1H, $J$ = 3.7 Hz; H-4), 3.70 (m, 4H, $NCH_2$); 1.70 (m, 6H, $CH_2$-). $^{13}$C NMR ($CDCl_3$) $\delta$ (ppm): 156.8 (C=O), 151.1 (C-5), 149.1 (C-2), 117.1 (C-4), 111.7 (C-3), 47.8 (C-2′), 44.3 (C6′), 26.7 (C-3′), 25.5 (C-5′), 24.4 (C-4′). EIHRMS calculated mass for $C_{10}H_{13}N_2O_4$ ($M + H^+$) 225.08698, found 225.08736

#### 4.4.13. 5-Nitro-furan-2-carboxylic acid benzylamide **(12)**

Solvent mixture for purification (Hexane/AcOEt, 70:30). Yield: 140 mg, 0.57 mmol, 89%. White crystalls, m.p. = 89.2–91.9 °C. IR (film) $\nu$ ($cm^{-1}$): 3296 (N-H), 3136 (CH alkene), 2929 (CH alkane), 1651 (C=C, C=O), 1556 (asymmetric C-N), 1485 (C=C furane), 1352 (symmetric C-N), 1286 (C-O), 1016 (C-H), 968 (C-N), 812, 738.$^1$H NMR ($CDCl_3$) $\delta$ (ppm): 7.38–7.28 (complex signal, 7H, Ar-H, H-3, H-4), 6.89 (br s, 1H, NH),4.64 (d, 2H, $J$ = 6.0 Hz, $CH_2$-Ar). $^{13}$C NMR ($CDCl_3$) $\delta$ (ppm): 156.3 (C=O amide), 151.2 (C-5), 148.0 (C-2), 137.1 (1-ArH), 128.9 (3,5-ArH), 128.0 (2,6-ArH), 127.9 (4-ArH), 116.1 (C-4), 112.5 (C-3), 43.6 (-$CH_2$Ar). EIHRMS calculated mass for $C_{12}H_{11}N_2O_4$ ($M + H^+$) 247.0713, found 247.0711.

#### 4.4.14. 5-Nitro-furan-2-carboxylic acid dibenzylamide **(13)**

Solvent mixture for purification (Hexane/AcOEt, 85:15). Yield: 151 mg, 0.45 mmol, 70%. Oil, Hex: EtOAc (85:15). IR (film) $\nu$ ($cm^{-1}$): 3132 (C-H furane), 3063, 3032 (C-H aromatic) 2924, 2851 (C-H alkane), 1736 (C=O), 1643 (asymmetric C-N), 1535 (C=C furane), 1350 (symmetric C-N), 1280, 1258 (C-O), 1018 (C-H), 968 (C-N), 814, 748, 702.$^1$H NMR ($CDCl_3$) $\delta$ (ppm): 7.37–7.26 (complex signal H-Ar), 7.28 (br s, 11H, Ar-H, H-3), 7.17 (d, 1H, $J$ = 3.8 Hz, H-4), 4.77 (br s, 2H, $CH_2$Ar), 4.71 (br s, 2H, $CH_2$Ar). $^{13}$C NMR ($CDCl_3$) $\delta$ (ppm): 158.6 (C=O amide), 151.4 (C-5), 148.4 (C-2), 136.5, 135.8 (1-ArH), 128.9 (3,5-ArH), 128.0 (2,6-ArH), 127.9 (4-ArH), 118.0 (C-4), 111.6 (C-3), 50.8, 49.4 ($CH_2$Ar). EIHRMS calculated mass for $C_{19}H_{16}N_2NaO_4$ ($M + Na^+$) 359.10078, found 359.10023.

### 4.5. Determination of TR activity

TR activity was measured by monitoring DTNB reduction at 405 nm ($\varepsilon$ = 13.8 $mM^{-1}cm^{-1}$ at 405 nm) by means of a coupled assay that guaranteed the oxidation of $T(SH)_2$ [41]. All enzyme assays were performed at 30 °C, in a final volume of 50 μl, and using a *Multiskan Ascent* one channel vertical light-path filter photometer (Thermo Electron Co.). The reaction mixture contained 100 mM Tris–HCl, pH 7.5, 2 mM EDTA, 200 μM NADPH, 4 nM *Tcr*TR, 10–100 μM $T(SH)_2$, 1 mM DTNB, and the respective nitrofuroic acid (5-NFA) based synthetic compound (1–100 μM). Reactions were started by addition of NADPH. As control assay, the 5-NFA related compounds were omitted in the reaction mixture. Kinetic constants are the means of at least three independent sets of data, and they were reproducible within ±10%.

### 4.6. Toxicity assays in cultures of T. cruzi epimastigotes

Suspensions of logarithmic-phase *T. cruzi* Dm28c epimastigotes at 1 × $10^6$ cell/ml were prepared in PBS plus 2% (w/v) glucose and transferred in aliquots of 200 μl to 96 well plates. Derivatives of the 5-NFA were added to different wells to get 0.1–100 μM final concentrations. The parasites were incubated for 24–48 h to evaluate epimastigote viability using resazurin assay [29]. Negative controls were performed replacing the addition of the inhibitors by an equal proportion of DMSO (solvent). As technical control, resazurin was incubated in the presence of each of the evaluated compounds (at different concentrations) but in the absence of parasites [29]. Calculated $IC_{50}$ values are the means of at least three independent experiments, which were reproduced within ±10%.

### 4.7. Toxicity assays in HeLa cell cultures

The toxicity of the synthetic compounds was determined using the crystal violet staining, as described elsewhere [42]. Cells were seeded at 2.5 × $10^4$ cell/well in 0.1 mL DMEM medium (supplemented with 2% fetal bovine serum) and incubated at 37 °C and 5% $CO_2$ during 24 h. Supernatants were discarded and renewed with fresh medium supplemented with the synthetic inhibitors. Eight serial dilutions of each compound were evaluated by duplicates. Cells were incubated for 24 h at 37 °C and 5% $CO_2$. The medium was discarded and cells were fixed and stained simultaneously with a solution of 0.75% (w/v) crystal violet in 40% (v/v) methanol. After 10 min, plates were washed with water and the remaining dye was solubilized in 20% (v/v) acetic acid. The plates were read at 540 nm with a microtiter plate reader. The signal intensity of each dilution was reported as the mean of the absorbance measured in triplicates. Untreated cells were considered as negative control. The non-toxic limit concentration was calculated as the concentration of compound which produced the same color intensity than that of the negative control.

### 4.8. Computational docking studies

The molecules **8**, **12**, and **13** along with Nfx were computationally tested (docked) against *Tcr*TR structure (pdb code: 1BZL (5)) in order to evaluate their in vitro activities and their theoretical

binding affinities. *Tcr*TR structure is a homodimer crystallized in complex with the oxidized form of the trypanothione molecule ($TS_2$) in a well known binding region [43] that is also found using different *in-silico* binding site predictors such as COACH [44], RaptorX Binding [45] and others (8,25,28). After the latter and also because we are interested in molecules that interfere the reductase activity, the region used to explore the possible binding modes (binding site) of these molecules was chosen to be the binding region of the $TS_2$. Docking simulations were performed using the AutoDock Vina 1.1.2 program [46]. Simulation parameters were chosen in a way ensuring a full coverage of the binding site, using a cubic search space of 24,389 $Å^3$ (29 Å × 29 Å x 29 Å) centered at mass center of the $TS_2$ molecule. The molecules were simulated as flexible while the protein was rigid. Since *Tcr*TR conforms a homodimers with two binding regions (one per subunit), these two regions were used for the docking simulations and each one was labeled as Region 1 (R1) located in chain A and Region 2 (R2) located in chain B. Furthermore, the docking simulation was done in the presence and absence of the $TS_2$ molecule, using the same search space. This allowed us to predict and analyze the binding affinity of synthetic inhibitors whether they joined into the same place of the substrate, or to the already bound $TS_2$ into the binding site. Therefore, the 4 molecules were docked on each region of the protein (8 dockings), with and without the $TS_2$ substrate (16 dockings) in both proteins.

## Acknowledgments

This work was supported by grants from UNL (CAI+D'11), CONICET (PIP112-2011-0100439, PIP114-2011-0100168, PIP GI 112-200801-00796), ANPCyT (PICT-2014-3256) and UNR (1BIO303 19/B450). PSF is fellows from CONICET. LEL is investigator from National University of Rosario (UNR). SAG, AAI, RMC, FEH, DR and DGA are investigator career members from CONICET.

## Appendix A. Supplementary data

Supplementary data related to this article can be found at http://dx.doi.org/10.1016/j.ejmech.2016.10.055.

## References

[1] T.N. Le, S.R. Meshnick, K. Kitchener, J.W. Eaton, A. Cerami, Iron-containing superoxide dismutase from Crithidia fasciculata. Purification, characterization, and similarity to Leishmanial and trypanosomal enzymes, J. Biol. Chem. 258 (1983) 125–130.
[2] H. Hillebrand, A. Schmidt, R.L. Krauth-Siegel, A second class of peroxidases linked to the trypanothione metabolism, J. Biol. Chem. 278 (2003) 6809–6815.
[3] T. Schlecker, A. Schmidt, N. Dirdjaja, F. Voncken, C. Clayton, R.L. Krauth-Siegel, Substrate specificity, localization, and essential role of the glutathione peroxidase-type tryparedoxin peroxidases in Trypanosoma brucei, J. Biol. Chem. 280 (2005) 14385–14394.
[4] B. Chance, H. Sies, A. Boveris, Hydroperoxide metabolism in mammalian organs, Physiol. Rev. 59 (1979) 527–605.
[5] A. Mezzetti, I.C. Di, A.M. Calafiore, A. Aceto, L. Marzio, G. Frederici, F. Cuccurullo, Glutathione peroxidase, glutathione reductase and glutathione transferase activities in the human artery, vein and heart, J. Mol. Cell Cardiol. 22 (1990) 935–938.
[6] A.H. Fairlamb, G.B. Henderson, A. Cerami, Trypanothione is the primary target for arsenical drugs against African trypanosomes, Proc. Natl. Acad. Sci. U. S. A. 86 (1989) 2607–2611.
[7] G.B. Henderson, A.H. Fairlamb, A. Cerami, Trypanothione dependent peroxide metabolism in Crithidia fasciculata and Trypanosoma brucei, Mol. Biochem. Parasitol. 24 (1987) 39–45.
[8] M.C. Jockers-Scherubl, R.H. Schirmer, R.L. Krauth-Siegel, Trypanothione reductase from Trypanosoma cruzi. Catalytic properties of the enzyme and inhibition studies with trypanocidal compounds, Eur. J. Biochem. 180 (1989) 267–272.
[9] R.L. Krauth-Siegel, B. Enders, G.B. Henderson, A.H. Fairlamb, R.H. Schirmer, Trypanothione reductase from Trypanosoma cruzi. Purification and characterization of the crystalline enzyme, Eur. J. Biochem. 164 (1987) 123–128.
[10] D.U. Gommel, E. Nogoceke, M. Morr, M. Kiess, H.M. Kalisz, L. Flohe, Catalytic characteristics of tryparedoxin, Eur. J. Biochem. 248 (1997) 913–918.
[11] S.A. Guerrero, L. Flohe, H.M. Kalisz, M. Montemartini, E. Nogoceke, H.J. Hecht, P. Steinert, M. Singh, Sequence, heterologous expression and functional characterization of tryparedoxin1 from Crithidia fasciculata, Eur. J. Biochem. 259 (1999) 789–794.
[12] S.A. Guerrero, J.A. Lopez, P. Steinert, M. Montemartini, H.M. Kalisz, W. Colli, M. Singh, M.J. Alves, L. Flohe, His-tagged tryparedoxin peroxidase of Trypanosoma cruzi as a tool for drug screening, Appl. Microbiol. Biotechnol. 53 (2000) 410–414.
[13] J.A. Lopez, T.U. Carvalho, S.W. de, L. Flohe, S.A. Guerrero, M. Montemartini, H.M. Kalisz, E. Nogoceke, M. Singh, M.J. Alves, W. Colli, Evidence for a trypanothione-dependent peroxidase system in Trypanosoma cruzi, Free Radic. Biol. Med. 28 (2000) 767–772.
[14] E. Nogoceke, D.U. Gommel, M. Kiess, H.M. Kalisz, L. Flohe, A unique cascade of oxidoreductases catalyses trypanothione-mediated peroxide metabolism in Crithidia fasciculata, Biol. Chem. 378 (1997) 827–836.
[15] S.R. Wilkinson, D.J. Meyer, J.M. Kelly, Biochemical characterization of a trypanosome enzyme with glutathione-dependent peroxidase activity, Biochem. J. 352 (2000) 755–761. Pt 3.
[16] R.P. Hirt, S. Muller, T.M. Embley, G.H. Coombs, The diversity and evolution of thioredoxin reductase: new perspectives, Trends Parasitol. 18 (2002) 302–308.
[17] S. Muller, E. Liebau, R.D. Walter, R.L. Krauth-Siegel, Thiol-based redox metabolism of protozoan parasites, Trends Parasitol. 19 (2003) 320–328.
[18] R. Friemann, H. Schmidt, S. Ramaswamy, M. Forstner, R.L. Krauth-Siegel, H. Eklund, Structure of thioredoxin from Trypanosoma brucei brucei, FEBS Lett. 554 (2003) 301–305.
[19] J. Alonso-Padilla, A. Rodriguez, High throughput screening for anti-Trypanosoma cruzi drug discovery, PLoS Negl. Trop. Dis. 8 (2014) e3259.
[20] J.R. Coura, Present situation and new strategies for Chagas disease chemotherapy: a proposal, Mem. Inst. Oswaldo Cruz 104 (2009) 549–554.
[21] J.A. Urbina, Recent clinical trials for the etiological treatment of chronic chagas disease: advances, challenges and perspectives, J. Eukaryot. Microbiol. 62 (2015) 149–156.
[22] M.V. Papadopoulou, W.D. Bloomer, H.S. Rosenzweig, I.P. O'Shea, S.R. Wilkinson, M. Kaiser, E. Chatelain, J.R. Ioset, Discovery of potent nitrotriazole-based antitrypanosomal agents: in vitro and in vivo evaluation, Bioorg Med. Chem. 23 (19) (2015) 6467–6476.
[23] M.V. Papadopoulou, W.D. Bloomer, H.S. Rosenzweig, S.R. Wilkinson, M. Kaiser, Novel nitro(triazole/imidazole)-based heteroarylamides/sulfonamides as potential antitrypanosomal agents, Eur. J. Med. Chem. 87 (2014) 79–88.
[24] M.V. Papadopoulou, W.D. Bloomer, G.I. Lepesheva, H.S. Rosenzweig, M. Kaiser, B. Aguilera-Venegas, S.R. Wilkinson, E. Chatelain, J.R. Ioset, Novel 3-nitrotriazole-based amides and carbinols as bifunctional antichagasic agents, J. Med. Chem. 58 (2015) 1307–1319.
[25] C. Bot, B.S. Hall, G. Alvarez, M.R. Di, M. Gonzalez, H. Cerecetto, S.R. Wilkinson, Evaluating 5-nitrofurans as trypanocidal agents, Antimicrob. Agents Chemother. 57 (2013) 1638–1647.
[26] S.R. Wilkinson, C. Bot, J.M. Kelly, B.S. Hall, Trypanocidal activity of nitroaromatic prodrugs: current treatments and future perspectives, Curr. Top. Med. Chem. 11 (2011) 2072–2084.
[27] B.S. Hall, C. Bot, S.R. Wilkinson, Nifurtimox activation by trypanosomal type I nitroreductases generates cytotoxic nitrile metabolites, J. Biol. Chem. 286 (2011) 13088–13095.
[28] S. Patterson, S. Wyllie, Nitro drugs for the treatment of trypanosomatid diseases: past, present, and future prospects, Trends Parasitol. 30 (2014) 289–298.
[29] V.E. Marquez, D.G. Arias, M.L. Chiribao, P. Faral-Tello, C. Robello, A.A. Iglesias, S.A. Guerrero, Redox metabolism in Trypanosoma cruzi. Biochemical characterization of dithiol glutaredoxin dependent cellular pathways, Biochimie 106 (2014) 56–67.
[30] C.S. Bond, Y. Zhang, M. Berriman, M.L. Cunningham, A.H. Fairlamb, W.N. Hunter, Crystal structure of Trypanosoma cruzi trypanothione reductase in complex with trypanothione, and the structure-based discovery of new natural product inhibitors, Structure 7 (1999) 81–89.
[31] Y. Zhang, C.S. Bond, S. Bailey, M.L. Cunningham, A.H. Fairlamb, W.N. Hunter, The crystal structure of trypanothione reductase from the human pathogen Trypanosoma cruzi at 2.3 A resolution, Protein Sci. 5 (1996) 52–61.
[32] Y. Zhang, S. Bailey, J.H. Naismith, C.S. Bond, J. Habash, P. McLaughlin, M.Z. Papiz, A. Borges, M. Cunningham, A.H. Fairlamb, Trypanosoma cruzi trypanothione reductase. Crystallization, unit cell dimensions and structure solution, J. Mol. Biol. 232 (1993) 1217–1220.
[33] S. Amari, M. Aizawa, J. Zhang, K. Fukuzawa, Y. Mochizuki, Y. Iwasawa, K. Nakata, H. Chuman, T. Nakano, VISCANA: visualized cluster analysis of protein-ligand interaction based on the ab initio fragment molecular orbital method for virtual ligand screening, J. Chem. Inf. Model 46 (2006) 221–230.
[34] J. Boyle, A visual environment for the manipulation and integration of JAVA beans, Bioinformatics 14 (1998) 739–748.
[35] D. Kozakov, R. Brenke, S.R. Comeau, S. Vajda, PIPER: an FFT-based protein docking program with pairwise potentials, Proteins 65 (2006) 392–406.
[36] S. Mishra, Computational prediction of protein-protein complexes, BMC Res. Notes 5 (2012) 495.
[37] J.D. Maya, C.O. Salas, B. Aguilera-Venegas, M.V. Diaz, R. Lopez-Munoz, Key proteins in the polyamine-trypanothione pathway as drug targets against Trypanosoma cruzi, Curr. Med. Chem. 21 (2014) 1757–1771.

[38] M.O. Khan, Trypanothione reductase: a viable chemotherapeutic target for antitrypanosomal and antileishmanial drug design, Drug Target Insights 2 (2007) 129–146.
[39] L. Salmon-Chemin, E. Buisine, V. Yardley, S. Kohler, M.A. Debreu, V. Landry, C. Sergheraert, S.L. Croft, R.L. Krauth-Siegel, E. Davioud-Charvet, 2- and 3-substituted 1,4-naphthoquinone derivatives as subversive substrates of trypanothione reductase and lipoamide dehydrogenase from Trypanosoma cruzi: synthesis and correlation between redox cycling activities and in vitro cytotoxicity, J. Med. Chem. 44 (2001) 548–565.
[40] M.L. Gomez, L. Erijman, S. Arauzo, H.N. Torres, M.T. Tellez-Inon, Protein kinase C in Trypanosoma cruzi epimastigote forms: partial purification and characterization, Mol. Biochem. Parasitol. 36 (1989) 101–108.
[41] M.F. Plano, R.M. Cravero, I. Nocito, E. Serra, S.A. Guerrero, D.G. Arias, Syntheses of a new class of phenyl butyraldehyde-derived amines with in vitro trypanocide activities, Med. Chem. Commun. 3 (2012) 225–228.
[42] K. Chiba, K. Kawakami, K. Tohyama, Simultaneous evaluation of cell viability by neutral red, MTT and crystal violet staining assays of the same cells, Toxicol Vitro 12 (1998) 251–258.
[43] J. Yang, A. Roy, Y. Zhang, BioLiP: a semi-manually curated database for biologically relevant ligand-protein interactions, Nucleic Acids Res. 41 (2013) D1096–D1103.
[44] J. Yang, A. Roy, Y. Zhang, Protein-ligand binding site recognition using complementary binding-specific substructure comparison and sequence profile alignment, Bioinformatics 29 (2013) 2588–2595.
[45] M. Kallberg, H. Wang, S. Wang, J. Peng, Z. Wang, H. Lu, J. Xu, Template-based protein structure modeling using the RaptorX web server, Nat. Protoc. 7 (2012) 1511–1522.
[46] O. Trott, A.J. Olson, AutoDock Vina: improving the speed and accuracy of docking with a new scoring function, efficient optimization, and multithreading, J. Comput. Chem. 31 (2010) 455–461.